

## PDF hosted at the Radboud Repository of the Radboud University Nijmegen

The following full text is a preprint version which may differ from the publisher's version.

For additional information about this publication click this link.

<http://hdl.handle.net/2066/124918>

Please be advised that this information was generated on 2019-04-25 and may be subject to change.

# Search for CP Violation in $Z^0 \longrightarrow \tau^+ \tau^-$ and an Upper Limit on the Weak Dipole Moment of the $\tau$ Lepton

The OPAL Collaboration

## Abstract

An improved test of  $\mathcal{CP}$  invariance in the reaction  $e^+ e^- \rightarrow \tau^+ \tau^-$  on the  $Z^0$  peak is performed using the data sample recorded between 1991 and 1995 with the OPAL detector at LEP. Optimal observables, requiring the reconstruction of the  $\tau$  flight direction and spin, have been used for different final state topologies. From the non-observation of  $\mathcal{CP}$  violation we derive 95% confidence level upper limits on the real and imaginary parts of the weak dipole moment of the  $\tau$  lepton of  $|\text{Re}(d_\tau^w(m_Z^2))| < 5.6 \times 10^{-18} e \text{ cm}$  and  $|\text{Im}(d_\tau^w(m_Z^2))| < 1.5 \times 10^{-17} e \text{ cm}$ , respectively.

(Submitted to Zeitschrift für Physik C)

# The OPAL Collaboration

K. Ackerstaff<sup>8</sup>, G. Alexander<sup>23</sup>, J. Allison<sup>16</sup>, N. Altekamp<sup>5</sup>, K. Ametewee<sup>25</sup>, K.J. Anderson<sup>9</sup>,  
S. Anderson<sup>12</sup>, S. Arcelli<sup>2</sup>, S. Asai<sup>24</sup>, D. Axen<sup>29</sup>, G. Azuelos<sup>18,a</sup>, A.H. Ball<sup>17</sup>, E. Barberio<sup>8</sup>,  
R.J. Barlow<sup>16</sup>, R. Bartoldus<sup>3</sup>, J.R. Batley<sup>5</sup>, J. Bechtluft<sup>14</sup>, C. Beeston<sup>16</sup>, T. Behnke<sup>8</sup>, A.N. Bell<sup>1</sup>,  
K.W. Bell<sup>20</sup>, G. Bella<sup>23</sup>, S. Bentvelsen<sup>8</sup>, P. Berlich<sup>10</sup>, S. Bethke<sup>14</sup>, O. Biebel<sup>14</sup>, A. Biguzzi<sup>2</sup>,  
V. Blobel<sup>27</sup>, I.J. Bloodworth<sup>1</sup>, J.E. Bloomer<sup>1</sup>, M. Bobinski<sup>10</sup>, P. Bock<sup>11</sup>, H.M. Bosch<sup>11</sup>,  
M. Boutemur<sup>34</sup>, B.T. Bouwens<sup>12</sup>, S. Braibant<sup>12</sup>, R.M. Brown<sup>20</sup>, H.J. Burckhart<sup>8</sup>, C. Burgard<sup>8</sup>,  
R. Bürgin<sup>10</sup>, P. Capiluppi<sup>2</sup>, R.K. Carnegie<sup>6</sup>, A.A. Carter<sup>13</sup>, J.R. Carter<sup>5</sup>, C.Y. Chang<sup>17</sup>,  
D.G. Charlton<sup>1,b</sup>, D. Chrisman<sup>4</sup>, P.E.L. Clarke<sup>15</sup>, I. Cohen<sup>23</sup>, J.E. Conboy<sup>15</sup>, O.C. Cooke<sup>16</sup>,  
M. Cuffiani<sup>2</sup>, S. Dado<sup>22</sup>, C. Dallapiccola<sup>17</sup>, G.M. Dallavalle<sup>2</sup>, S. De Jong<sup>12</sup>, L.A. del Pozo<sup>8</sup>, K. Desch<sup>3</sup>,  
M.S. Dixit<sup>7</sup>, E. do Couto e Silva<sup>12</sup>, M. Doucet<sup>18</sup>, E. Duchovni<sup>26</sup>, G. Duckeck<sup>34</sup>, I.P. Duerdoth<sup>16</sup>,  
J.E.G. Edwards<sup>16</sup>, P.G. Estabrooks<sup>6</sup>, H.G. Evans<sup>9</sup>, M. Evans<sup>13</sup>, F. Fabbri<sup>2</sup>, P. Fath<sup>11</sup>, F. Fiedler<sup>27</sup>,  
M. Fierro<sup>2</sup>, H.M. Fischer<sup>3</sup>, R. Folman<sup>26</sup>, D.G. Fong<sup>17</sup>, M. Foucher<sup>17</sup>, A. Fürtjes<sup>8</sup>, P. Gagnon<sup>7</sup>,  
A. Gaidot<sup>21</sup>, J.W. Gary<sup>4</sup>, J. Gascon<sup>18</sup>, S.M. Gascon-Shotkin<sup>17</sup>, N.I. Geddes<sup>20</sup>, C. Geich-Gimbel<sup>3</sup>,  
F.X. Gentit<sup>21</sup>, T. Geralis<sup>20</sup>, G. Giacomelli<sup>2</sup>, P. Giacomelli<sup>4</sup>, R. Giacomelli<sup>2</sup>, V. Gibson<sup>5</sup>,  
W.R. Gibson<sup>13</sup>, D.M. Gingrich<sup>30,a</sup>, D. Glenzinski<sup>9</sup>, J. Goldberg<sup>22</sup>, M.J. Goodrick<sup>5</sup>, W. Gorn<sup>4</sup>,  
C. Grandi<sup>2</sup>, E. Gross<sup>26</sup>, J. Grunhaus<sup>23</sup>, M. Gruwé<sup>8</sup>, C. Hajdu<sup>32</sup>, G.G. Hanson<sup>12</sup>, M. Hansroul<sup>8</sup>,  
M. Hapke<sup>13</sup>, C.K. Hargrove<sup>7</sup>, P.A. Hart<sup>9</sup>, C. Hartmann<sup>3</sup>, M. Hauschild<sup>8</sup>, C.M. Hawkes<sup>5</sup>, R. Hawkings<sup>8</sup>,  
R.J. Hemingway<sup>6</sup>, M. Herndon<sup>17</sup>, G. Herten<sup>10</sup>, R.D. Heuer<sup>8</sup>, M.D. Hildreth<sup>8</sup>, J.C. Hill<sup>5</sup>, S.J. Hillier<sup>1</sup>,  
T. Hilse<sup>10</sup>, P.R. Hobson<sup>25</sup>, R.J. Homer<sup>1</sup>, A.K. Honma<sup>28,a</sup>, D. Horváth<sup>32,c</sup>, R. Howard<sup>29</sup>,  
R.E. Hughes-Jones<sup>16</sup>, D.E. Hutchcroft<sup>5</sup>, P. Igo-Kemenes<sup>11</sup>, D.C. Imrie<sup>25</sup>, M.R. Ingram<sup>16</sup>, K. Ishii<sup>24</sup>,  
A. Jawahery<sup>17</sup>, P.W. Jeffreys<sup>20</sup>, H. Jeremie<sup>18</sup>, M. Jimack<sup>1</sup>, A. Joly<sup>18</sup>, C.R. Jones<sup>5</sup>, G. Jones<sup>16</sup>,  
M. Jones<sup>6</sup>, R.W.L. Jones<sup>8</sup>, U. Jost<sup>11</sup>, P. Jovanovic<sup>1</sup>, T.R. Junk<sup>8</sup>, D. Karlen<sup>6</sup>, K. Kawagoe<sup>24</sup>,  
T. Kawamoto<sup>24</sup>, R.K. Keeler<sup>28</sup>, R.G. Kellogg<sup>17</sup>, B.W. Kennedy<sup>20</sup>, B.J. King<sup>8</sup>, J. Kirk<sup>29</sup>, S. Kluth<sup>8</sup>,  
T. Kobayashi<sup>24</sup>, M. Kobel<sup>10</sup>, D.S. Koetke<sup>6</sup>, T.P. Kokott<sup>3</sup>, M. Kolrep<sup>10</sup>, S. Komamiya<sup>24</sup>, T. Kress<sup>11</sup>,  
P. Krieger<sup>6</sup>, J. von Krogh<sup>11</sup>, P. Kyberd<sup>13</sup>, G.D. Lafferty<sup>16</sup>, H. Lafoux<sup>21</sup>, R. Lahmann<sup>17</sup>, W.P. Lai<sup>19</sup>,  
D. Lanske<sup>14</sup>, J. Lauber<sup>15</sup>, S.R. Lautenschlager<sup>31</sup>, J.G. Layter<sup>4</sup>, D. Lazic<sup>22</sup>, A.M. Lee<sup>31</sup>, E. Lefebvre<sup>18</sup>,  
D. Lellouch<sup>26</sup>, J. Letts<sup>2</sup>, L. Levinson<sup>26</sup>, C. Lewis<sup>15</sup>, S.L. Lloyd<sup>13</sup>, F.K. Loebinger<sup>16</sup>, G.D. Long<sup>17</sup>,  
M.J. Losty<sup>7</sup>, J. Ludwig<sup>10</sup>, A. Malik<sup>21</sup>, M. Mannelli<sup>8</sup>, S. Marcellini<sup>2</sup>, C. Markus<sup>3</sup>, A.J. Martin<sup>13</sup>,  
J.P. Martin<sup>18</sup>, G. Martinez<sup>17</sup>, T. Mashimo<sup>24</sup>, W. Matthews<sup>25</sup>, P. Mättig<sup>3</sup>, W.J. McDonald<sup>30</sup>,  
J. McKenna<sup>29</sup>, E.A. Mckigney<sup>15</sup>, T.J. McMahon<sup>1</sup>, A.I. McNab<sup>13</sup>, R.A. McPherson<sup>8</sup>, F. Meijers<sup>8</sup>,  
S. Menke<sup>3</sup>, F.S. Merritt<sup>9</sup>, H. Mes<sup>7</sup>, J. Meyer<sup>27</sup>, A. Michelini<sup>2</sup>, G. Mikenberg<sup>26</sup>, D.J. Miller<sup>15</sup>, R. Mir<sup>26</sup>,  
W. Mohr<sup>10</sup>, A. Montanari<sup>2</sup>, T. Mori<sup>24</sup>, M. Morii<sup>24</sup>, U. Müller<sup>3</sup>, K. Nagai<sup>26</sup>, I. Nakamura<sup>24</sup>, H.A. Neal<sup>8</sup>,  
B. Nellen<sup>3</sup>, B. Nijhar<sup>16</sup>, R. Nisius<sup>8</sup>, S.W. O'Neale<sup>1</sup>, F.G. Oakham<sup>7</sup>, F. Odorici<sup>2</sup>, H.O. Ogren<sup>12</sup>,  
N.J. Oldershaw<sup>16</sup>, T. Omori<sup>24</sup>, M.J. Oreglia<sup>9</sup>, S. Orito<sup>24</sup>, J. Pálinkás<sup>33,d</sup>, G. Pásztor<sup>32</sup>, J.R. Pater<sup>16</sup>,  
G.N. Patrick<sup>20</sup>, J. Patt<sup>10</sup>, M.J. Pearce<sup>1</sup>, S. Petzold<sup>27</sup>, P. Pfeifenschneider<sup>14</sup>, J.E. Pilcher<sup>9</sup>, J. Pinfold<sup>30</sup>,  
D.E. Plane<sup>8</sup>, P. Poffenberger<sup>28</sup>, B. Poli<sup>2</sup>, A. Posthaus<sup>3</sup>, H. Przysiezniak<sup>30</sup>, D.L. Rees<sup>1</sup>, D. Rigby<sup>1</sup>,  
S. Robertson<sup>28</sup>, S.A. Robins<sup>13</sup>, N. Rodning<sup>30</sup>, J.M. Roney<sup>28</sup>, A. Rooke<sup>15</sup>, E. Ros<sup>8</sup>, A.M. Rossi<sup>2</sup>,  
M. Rosvick<sup>28</sup>, P. Routenburg<sup>30</sup>, Y. Rozen<sup>22</sup>, K. Runge<sup>10</sup>, O. Runolfsson<sup>8</sup>, U. Ruppel<sup>14</sup>, D.R. Rust<sup>12</sup>,  
R. Rylko<sup>25</sup>, K. Sachs<sup>10</sup>, E.K.G. Sarkisyan<sup>23</sup>, M. Sasaki<sup>24</sup>, C. Sbarra<sup>2</sup>, A.D. Schaile<sup>34</sup>, O. Schaile<sup>34</sup>,  
F. Scharf<sup>8</sup>, P. Scharff-Hansen<sup>8</sup>, P. Schenk<sup>27</sup>, B. Schmitt<sup>8</sup>, S. Schmitt<sup>11</sup>, M. Schröder<sup>8</sup>,  
H.C. Schultz-Coulon<sup>10</sup>, M. Schulz<sup>8</sup>, M. Schumacher<sup>3</sup>, P. Schütz<sup>3</sup>, W.G. Scott<sup>20</sup>, T.G. Shears<sup>16</sup>,  
B.C. Shen<sup>4</sup>, C.H. Shepherd-Themistocleous<sup>8</sup>, P. Sherwood<sup>15</sup>, G.P. Siroli<sup>2</sup>, A. Sittler<sup>27</sup>, A. Skillman<sup>15</sup>,  
A. Skuja<sup>17</sup>, A.M. Smith<sup>8</sup>, T.J. Smith<sup>28</sup>, G.A. Snow<sup>17</sup>, R. Sobie<sup>28</sup>, S. Söldner-Rembold<sup>10</sup>,  
R.W. Springer<sup>30</sup>, M. Sproston<sup>20</sup>, A. Stahl<sup>3</sup>, M. Steiert<sup>11</sup>, K. Stephens<sup>16</sup>, J. Steuerer<sup>27</sup>,  
B. Stockhausen<sup>3</sup>, D. Strom<sup>19</sup>, F. Strumia<sup>8</sup>, P. Szymanski<sup>20</sup>, R. Taffrou<sup>18</sup>, S.D. Talbot<sup>1</sup>, S. Tanaka<sup>24</sup>,  
P. Taras<sup>18</sup>, S. Tarem<sup>22</sup>, M. Thiergen<sup>10</sup>, M.A. Thomson<sup>8</sup>, E. von Törne<sup>3</sup>, S. Towers<sup>6</sup>, I. Trigger<sup>18</sup>,  
T. Tsukamoto<sup>24</sup>, E. Tsur<sup>23</sup>, A.S. Turcot<sup>9</sup>, M.F. Turner-Watson<sup>8</sup>, P. Utzat<sup>11</sup>, R. Van Kooten<sup>12</sup>,  
G. Vasseur<sup>21</sup>, M. Verzocchi<sup>10</sup>, P. Vikas<sup>18</sup>, M. Vinciter<sup>28</sup>, E.H. Vokurka<sup>16</sup>, F. Wäckerle<sup>10</sup>, A. Wagner<sup>27</sup>,  
C.P. Ward<sup>5</sup>, D.R. Ward<sup>5</sup>, J.J. Ward<sup>15</sup>, P.M. Watkins<sup>1</sup>, A.T. Watson<sup>1</sup>, N.K. Watson<sup>7</sup>, P.S. Wells<sup>8</sup>,

N. Vermes<sup>3</sup>, J.S. White<sup>28</sup>, B. Wilkens<sup>10</sup>, G.W. Wilson<sup>27</sup>, J.A. Wilson<sup>1</sup>, G. Wolf<sup>26</sup>, S. Wotton<sup>5</sup>,  
T.R. Wyatt<sup>16</sup>, S. Yamashita<sup>24</sup>, G. Yekutieli<sup>26</sup>, V. Zacek<sup>18</sup>

- <sup>1</sup>School of Physics and Space Research, University of Birmingham, Birmingham B15 2TT, UK  
<sup>2</sup>Dipartimento di Fisica dell' Università di Bologna and INFN, I-40126 Bologna, Italy  
<sup>3</sup>Physikalisches Institut, Universität Bonn, D-53115 Bonn, Germany  
<sup>4</sup>Department of Physics, University of California, Riverside CA 92521, USA  
<sup>5</sup>Cavendish Laboratory, Cambridge CB3 0HE, UK  
<sup>6</sup>Ottawa-Carleton Institute for Physics, Department of Physics, Carleton University, Ottawa, Ontario K1S 5B6, Canada  
<sup>7</sup>Centre for Research in Particle Physics, Carleton University, Ottawa, Ontario K1S 5B6, Canada  
<sup>8</sup>CERN, European Organisation for Particle Physics, CH-1211 Geneva 23, Switzerland  
<sup>9</sup>Enrico Fermi Institute and Department of Physics, University of Chicago, Chicago IL 60637, USA  
<sup>10</sup>Fakultät für Physik, Albert Ludwigs Universität, D-79104 Freiburg, Germany  
<sup>11</sup>Physikalisches Institut, Universität Heidelberg, D-69120 Heidelberg, Germany  
<sup>12</sup>Indiana University, Department of Physics, Swain Hall West 117, Bloomington IN 47405, USA  
<sup>13</sup>Queen Mary and Westfield College, University of London, London E1 4NS, UK  
<sup>14</sup>Technische Hochschule Aachen, III Physikalisches Institut, Sommerfeldstrasse 26-28, D-52056 Aachen, Germany  
<sup>15</sup>University College London, London WC1E 6BT, UK  
<sup>16</sup>Department of Physics, Schuster Laboratory, The University, Manchester M13 9PL, UK  
<sup>17</sup>Department of Physics, University of Maryland, College Park, MD 20742, USA  
<sup>18</sup>Laboratoire de Physique Nucléaire, Université de Montréal, Montréal, Quebec H3C 3J7, Canada  
<sup>19</sup>University of Oregon, Department of Physics, Eugene OR 97403, USA  
<sup>20</sup>Rutherford Appleton Laboratory, Chilton, Didcot, Oxfordshire OX11 0QX, UK  
<sup>21</sup>CEA, DAPNIA/SPP, CE-Saclay, F-91191 Gif-sur-Yvette, France  
<sup>22</sup>Department of Physics, Technion-Israel Institute of Technology, Haifa 32000, Israel  
<sup>23</sup>Department of Physics and Astronomy, Tel Aviv University, Tel Aviv 69978, Israel  
<sup>24</sup>International Centre for Elementary Particle Physics and Department of Physics, University of Tokyo, Tokyo 113, and Kobe University, Kobe 657, Japan  
<sup>25</sup>Brunel University, Uxbridge, Middlesex UB8 3PH, UK  
<sup>26</sup>Particle Physics Department, Weizmann Institute of Science, Rehovot 76100, Israel  
<sup>27</sup>Universität Hamburg/DESY, II Institut für Experimental Physik, Notkestrasse 85, D-22607 Hamburg, Germany  
<sup>28</sup>University of Victoria, Department of Physics, P O Box 3055, Victoria BC V8W 3P6, Canada  
<sup>29</sup>University of British Columbia, Department of Physics, Vancouver BC V6T 1Z1, Canada  
<sup>30</sup>University of Alberta, Department of Physics, Edmonton AB T6G 2J1, Canada  
<sup>31</sup>Duke University, Dept of Physics, Durham, NC 27708-0305, USA  
<sup>32</sup>Research Institute for Particle and Nuclear Physics, H-1525 Budapest, P O Box 49, Hungary  
<sup>33</sup>Institute of Nuclear Research, H-4001 Debrecen, P O Box 51, Hungary  
<sup>34</sup>Ludwigs-Maximilians-Universität München, Sektion Physik, Am Coulombwall 1, D-85748 Garching, Germany

<sup>a</sup> and at TRIUMF, Vancouver, Canada V6T 2A3

<sup>b</sup> and Royal Society University Research Fellow

<sup>c</sup> and Institute of Nuclear Research, Debrecen, Hungary

<sup>d</sup> and Department of Experimental Physics, Lajos Kossuth University, Debrecen, Hungary

# 1 Introduction

$\mathcal{CP}$  violation, where  $\mathcal{C}$  denotes charge conjugation and  $\mathcal{P}$  the parity transformation, is one of the necessary ingredients to describe the baryon asymmetry in the universe [1]. Its understanding is one of the main challenges of elementary particle physics today. So far, a manifestation of  $\mathcal{CP}$  violation has only been found in the decays of neutral kaons [2]. In the Standard Model of electroweak interactions  $\mathcal{CP}$  violation is introduced by a complex phase in the quark mixing (CKM) matrix [3]. This description will be studied in the b-quark sector in the near future by several experiments. It is, however, not yet clear if  $\mathcal{CP}$  violation as described by the Standard Model can also explain the observed baryon asymmetry in the universe or if additional sources of  $\mathcal{CP}$  violation must be introduced [4].

Experimentally it is instructive to test the Standard Model (SM) by looking for new  $\mathcal{CP}$  phenomena studying reactions for which the Standard Model does not predict any measurable effect. For the production of fermion pairs through  $Z^0$  exchange the  $\mathcal{CP}$  violating amplitudes of the Standard Model, governed by higher-order corrections involving CKM phases, have been estimated to be less than  $10^{-7} \times T_{SM}$  [5], where  $T_{SM}$  denotes the Standard Model amplitude. An observation of  $\mathcal{CP}$  violation in  $Z^0 \rightarrow f\bar{f}$  would therefore indicate new physics beyond the Standard Model.

There are several advantages in using the decay  $Z^0 \rightarrow \tau^+ \tau^-$  to test  $\mathcal{CP}$  invariance. Firstly, in many  $\mathcal{CP}$  violating extensions of the Standard Model the new couplings parametrized by  $\mathcal{P}$  and  $\mathcal{T}$  (time reversal) violating dipole moments of the fermions are proportional to the masses of the fermions involved. This occurs because chirality flipping form factors are required for a  $\mathcal{CP}$  violating interaction. In multi-Higgs models [6] the magnitude of the dipole moment  $d$  of heavy fermions scales with the third power<sup>1</sup> of the fermion mass,  $d_f \propto m_f^3$ , while leptoquark models [8] predict the ratio of the lepton dipole moments to be  $d_\tau : d_\mu : d_e = m_\tau m_t^3 : m_\mu m_c^2 : m_e m_u^2$ . Secondly, to be sensitive to a  $\mathcal{CP}$  asymmetry the spin correlations of the final state fermions must be measured. For the case of leptons this is most easily accessible for the short lived  $\tau$  for which information about the spins can be extracted from the four-momenta of the  $\tau$  decay products.

New  $\mathcal{CP}$  violating physics can be described by an effective Lagrangian in a model independent way as suggested by Bernreuther et al. [5]. The strength of the new interaction is governed by electric and weak dipole form factors which are, most generally, complex. Neglecting the contribution from one-photon annihilation at the  $Z^0$  peak this ansatz has only one parameter,  $d_\tau^w(m_Z^2)$ , termed the weak dipole moment of the  $\tau$  lepton. At the Born level,  $\mathcal{CP}$  violation arises from the interference of the SM amplitude  $T_{SM}$  with the  $\mathcal{CP}$  violating amplitude  $T_{\mathcal{CP}}$ . Only the interference term is  $\mathcal{CP}$ -odd. The  $\mathcal{CP}$ -even  $|T_{\mathcal{CP}}|^2$  is of order  $|d_\tau^w(m_Z^2)|^2$  and contributes to the partial width  $Z^0 \rightarrow \tau^+ \tau^-$  [5], a fact which can also be used to determine  $|d_\tau^w(m_Z^2)|$ . This, however, does not constitute a test of  $\mathcal{CP}$  invariance. The interference term can be split into two parts,  $2\text{Re}(T_{SM}^* T_{\mathcal{CP}}) = \text{Re}(d_\tau^w) \mathcal{M}_{\mathcal{CP}}^{\text{Re}} + \text{Im}(d_\tau^w) \mathcal{M}_{\mathcal{CP}}^{\text{Im}}$ , which are proportional to the real and imaginary parts of the weak dipole moment, respectively. The squared matrix elements,  $\mathcal{M}_{\mathcal{CP}}^{\text{Re}}$  and  $\mathcal{M}_{\mathcal{CP}}^{\text{Im}}$ , are further explained below. Contributions to the imaginary part of  $d_\tau^w$  are related to absorptive parts in the  $\mathcal{CP}$  violating interaction. A more detailed discussion on the formalism can be found in [9].

Direct tests of  $\mathcal{CP}$  invariance in  $e^+e^- \rightarrow \tau^+ \tau^-$  exploiting the interference term have so far been published by OPAL [10, 11] and ALEPH [12], leading to upper limits on the weak dipole moment. In ref. [11] optimal observables were used for the first time to set limits on the real and imaginary parts of  $d_\tau^w(m_Z^2)$  separately. In this paper we present an analysis which is similar to that of ref. [11] but includes several improvements resulting in a greater sensitivity. For the most of the data sample the implementation of a new microvertex detector [13] allows the full reconstruction of the  $\tau$  flight direction for hadronic  $\tau$  decays without neutral hadrons in the final state. A new reconstruction algorithm for photons and neutral pions has been used to improve the identification of the various decay modes of the  $\tau$ . Finally, the event sample has more than doubled. We restrict the present discussion to the main improvements with respect to the previously published results [11] to which we also refer for further details.

---

<sup>1</sup>For light fermions the dominant contribution to  $d$  is a two-loop effect [7].

## 2 Determination of $d_\tau^w$ using Optimal $\mathcal{CP}$ -odd Observables

$\mathcal{CP}$  invariance of the  $\tau$ -pair production process at LEP is tested using  $\mathcal{CP}$ -odd observables constructed from the measured momenta and energies of the  $\tau$  decay products. If  $\tau$ -pair production respects  $\mathcal{CP}$  symmetry then the expectation values of these observables must vanish, i.e.  $\langle \mathcal{O} \rangle = 0$ . Any significant observed deviation from zero implies  $\mathcal{CP}$  violation.

$\mathcal{CP}$ -odd observables differ from each other by their transformation property under time reversal  $T$ . The mean values of  $\mathcal{CP}$ - and  $T$ -odd observables,  $\langle \mathcal{O}^{T-} \rangle$ , are proportional to  $\text{Re}(d_\tau^w)$  and those of  $\mathcal{CP}$ -odd and  $T$ -even ones,  $\langle \mathcal{O}^{T+} \rangle$ , to  $\text{Im}(d_\tau^w)$ :

$$\langle \mathcal{O}^{T-} \rangle_{AB} = \langle \mathcal{O}^{\text{Re}} \rangle_{AB} = \frac{m_Z}{e} \cdot c_{AB} \cdot \text{Re}(d_\tau^w) \quad (1)$$

$$\langle \mathcal{O}^{T+} \rangle_{AB} = \langle \mathcal{O}^{\text{Im}} \rangle_{AB} = \frac{m_Z}{e} \cdot f_{AB} \cdot \text{Im}(d_\tau^w) \quad , \quad (2)$$

where  $e$  denotes the magnitude of the electron charge.

The dimensionless constants  $c_{AB}$  and  $f_{AB}$ , henceforth called sensitivities, differ for the specific decay channels of the taus, A and B. In the early analyses [10, 12]  $\mathcal{CP}$ -odd observables termed  $T_{33}$  or  $\hat{T}_{33}$  were constructed from the momenta and energies of the final state particles. Optimal observables [14, 15, 16] allow the measurement of the weak dipole moment with the highest statistical precision by maximizing the signal-to-noise ratio. Neglecting contributions of order  $|d_\tau^w|^2$  in the cross-section, the optimal observables are given by:

$$\mathcal{O}^{\text{Re}} = \frac{\mathcal{M}_{\mathcal{CP}}^{\text{Re}}}{\mathcal{M}_{SM}} \quad , \quad \mathcal{O}^{\text{Im}} = \frac{\mathcal{M}_{\mathcal{CP}}^{\text{Im}}}{\mathcal{M}_{SM}} \quad . \quad (3)$$

Here  $\mathcal{M}_{SM}$  denotes the squared Standard Model matrix element and  $\mathcal{M}_{\mathcal{CP}}^{\text{Re}}$  and  $\mathcal{M}_{\mathcal{CP}}^{\text{Im}}$  are the  $\mathcal{CP}$  violating contributions to the squared amplitude as mentioned in the introduction. The computation of  $\mathcal{M}_{SM}$ ,  $\mathcal{M}_{\mathcal{CP}}^{\text{Re}}$  and  $\mathcal{M}_{\mathcal{CP}}^{\text{Im}}$  requires an estimation of the  $\tau$  flight and spin directions for which analytic expressions [17] are given in the appendix. It has been shown [16] that the mean value of the distribution of the observables  $\langle \mathcal{O} \rangle$  contains the maximum information on the weak dipole moment.

## 3 Event Selection

The data were collected with the OPAL detector at LEP between 1991 and 1995 at centre of mass energies around the  $Z^0$  peak and correspond to an integrated luminosity of  $153 \text{ pb}^{-1}$  or about 190000 produced  $\tau$ -pair events. A detailed description of the detector is given elsewhere [13, 18, 19]. Because the event selection efficiency and purity for the various  $\tau$  decay modes and also the sensitivities depend on  $\cos\theta$ , where  $\theta$  is the angle between the event thrust axis and the beam, the solid angle of the detector has been divided into three regions, termed ‘barrel’ ( $|\cos\theta| < 0.68$ ), ‘overlap’ ( $0.68 < |\cos\theta| < 0.76$ ), and ‘endcaps’ ( $0.76 < |\cos\theta| < 0.95$ ).

The event selection is performed in two steps. First,  $\tau$ -pairs are selected from the  $Z^0$  decays and second, decay modes are assigned independently to each of the two  $\tau$  leptons per event. Neglecting initial and final state radiation the two  $\tau$ 's are produced back-to-back with an energy equal to the beam energy. The typical event topology therefore is that of two narrow particle jets of low multiplicity in opposite hemispheres. Two cones with an opening angle of  $35^\circ$  around the centre of the  $\tau$  jets, defined by the thrust axis, usually contain all particles from the  $\tau$  decay. Tau pairs have been selected using the procedure as described in [20], but in addition exactly two cones with net charges  $-1$  and  $+1$ , and a total momentum of less than 90% of the centre of mass energy have been demanded to reject  $\mu$ -pair and Bhabha scattering events. Only 1-1, 1-3 and 3-3 track topologies have been considered.

Each  $\tau$  cone is independently analysed to classify its decay mode. A maximum likelihood method is employed to identify the various  $\tau$  decay channels as described in [11]. Only events where both tau candidates are identified as one of the following decay modes are kept:

$$\tau \xrightarrow{1\text{-prong}} \nu_\tau + e\nu_e, \mu\nu_\mu, \pi(K), \pi(K)\pi^0 \quad \text{or} \quad \tau \xrightarrow{3\text{-prong}} \nu_\tau + 3\pi.$$

Largely the same variables as described in [11] have been used with some improvements. In the 1-prong case observables used in the likelihood include the total energy in the cone observed in the electromagnetic calorimeter (ECAL) divided by the track momentum, the ECAL energy unassociated with the charged track and electromagnetic cluster shapes as seen in the ECAL and the presampler. The number and energies of photon candidates, constructed using the Maximum Entropy Method [21], as well as invariant masses calculated from various combinations of these photon candidates and the charged track were used to define additional likelihood variables. Finally, the ionization energy loss of the charged track seen in the tracking detector (dE/dx) and the number of hits in the outer regions of the HCAL and the muon chambers were also used in the likelihood.

For 3-prong decays the likelihood was constructed including variables based on the total energy in the cone observed in the ECAL divided by the sum of the track momenta, the probability for each track in the cone to be a pion or an electron derived from dE/dx measurements, the quality of a fit of the three tracks to a common vertex and the sum of the energies of any photon candidates, defined as described above, not associated to a charged track.

Table 1 shows the probabilities of classifying a certain decay channel as one of the channels considered. Note that the row and column sums do not add up to one because the table does not contain all the channels considered in the likelihood classification. Photon conversions are, for example, omitted from the table.

| Monte-Carlo<br>$\tau$ decay channel | identification probabilities (%) |       |       |             |                        |       |       |             |                        |       |       |             |
|-------------------------------------|----------------------------------|-------|-------|-------------|------------------------|-------|-------|-------------|------------------------|-------|-------|-------------|
|                                     | barrel                           |       |       |             | overlap                |       |       |             | endcaps                |       |       |             |
| 1-prong                             | $e$                              | $\mu$ | $\pi$ | $\rho$      | $e$                    | $\mu$ | $\pi$ | $\rho$      | $e$                    | $\mu$ | $\pi$ | $\rho$      |
| $e$                                 | 95.3                             | 0.0   | 0.4   | 1.2         | 94.6                   | 0.0   | 0.7   | 1.5         | 89.2                   | 0.0   | 1.3   | 2.5         |
| $\mu$                               | 0.5                              | 92.3  | 1.0   | 0.6         | 0.5                    | 90.5  | 3.0   | 0.6         | 0.1                    | 89.8  | 3.3   | 0.7         |
| $\pi$                               | 1.6                              | 2.3   | 78.0  | 9.6         | 3.2                    | 4.7   | 69.4  | 13.7        | 2.8                    | 6.0   | 68.9  | 11.9        |
| $\rho$                              | 0.3                              | 0.2   | 7.8   | 61.4        | 0.3                    | 0.2   | 8.6   | 57.9        | 0.7                    | 0.2   | 10.7  | 48.6        |
| $a_1 \rightarrow \pi 2\pi^0$        | 0.0                              | 0.0   | 0.7   | 21.9        | 0.0                    | 0.0   | 1.3   | 24.7        | 0.2                    | 0.0   | 1.8   | 19.1        |
| 3-prong                             | $a_1 \rightarrow 3\pi$           |       |       | $3\pi\pi^0$ | $a_1 \rightarrow 3\pi$ |       |       | $3\pi\pi^0$ | $a_1 \rightarrow 3\pi$ |       |       | $3\pi\pi^0$ |
| $a_1 \rightarrow 3\pi$              | 69.2                             |       |       | 11.7        | 69.0                   |       |       | 12.7        | 60.2                   |       |       | 11.5        |
| $3\pi\pi^0$                         | 23.6                             |       |       | 47.4        | 27.1                   |       |       | 43.3        | 21.2                   |       |       | 36.0        |

Table 1: Identification probabilities of the maximum likelihood selection.

Accurate knowledge of the purities and misidentification probabilities is important for the determination of the sensitivities (see section 5). The uncertainties arising from disagreements between the detector simulation and the data are estimated by comparing reference distributions for the various decay channels for data and Monte Carlo. The data reference samples were created making no use of the information from the detector component which provided the variable to be checked. The systematic errors on the purities were then estimated by reweighting the reference distributions forcing agreement with the data. The full difference in the purities when comparing the decay mode identification with unsmearred and with smearred reference distributions has been accounted for in the systematic error on the purities (c.f. table 2).

The contribution of non- $\tau$  background in the different decay channels and detector regions is determined by Monte Carlo studies. The background in the 1-3 and 3-3 topologies is less than 0.5%, mostly coming from multihadron events. In 1-1 topologies containing hadrons the background is typically (0.2 - 4.2)% rising up to 20% for fully leptonic 1-1 events in the endcaps. The influence of the background and its impact on the different decay channels and detector regions has been taken into account in calculating the sensitivities (see section 5). The results are found to be insensitive to variations in the non- $\tau$  background of  $\pm 100\%$ .

| decay channel                 | purity (%)             |                        |                        |
|-------------------------------|------------------------|------------------------|------------------------|
|                               | barrel                 | overlap                | endcaps                |
| $\tau \rightarrow \nu_\tau +$ |                        |                        |                        |
| $e \nu_e$                     | $97.7 \pm 0.1 \pm 0.1$ | $96.8 \pm 0.3 \pm 0.2$ | $96.8 \pm 0.2 \pm 0.3$ |
| $\mu \nu_\mu$                 | $97.8 \pm 0.1 \pm 0.1$ | $96.3 \pm 0.4 \pm 0.2$ | $95.3 \pm 0.2 \pm 1.2$ |
| $\pi (K)$                     | $78.3 \pm 0.5 \pm 1.4$ | $71.8 \pm 1.1 \pm 0.8$ | $66.7 \pm 0.5 \pm 0.9$ |
| $\rho (K^*)$                  | $82.4 \pm 0.4 \pm 0.3$ | $78.6 \pm 0.8 \pm 0.5$ | $77.0 \pm 0.5 \pm 0.8$ |
| $a_1^{3\text{-prong}}$        | $77.2 \pm 0.5 \pm 1.0$ | $75.2 \pm 1.3 \pm 0.8$ | $75.5 \pm 0.8 \pm 3.3$ |

Table 2: Purities of the maximum likelihood selection for identified  $\tau$  pairs. The first error denotes the uncertainty due to the limited Monte Carlo statistics, the second error arises from the effect of the smearing.

## 4 Tau Flight and Tau Spin Directions

The  $\tau$  flight direction cannot usually be measured directly because at least one unobserved neutrino appears in the decay. However, in the case of two-body  $\tau$  decays and under the assumption of back-to-back  $\tau$ -pair production, one can reconstruct the direction of the parent  $\tau$  from the four-momenta of the  $\tau$  daughter particles up to a twofold ambiguity [22]. Three different cases must be considered in the reconstruction (see appendix B): (a) both taus decay to charged hadrons only, (b) the taus decay to hadrons with at least one neutral hadron, and (c) at least one tau decays to leptons only. In case (a) the  $\tau$  flight direction can be completely reconstructed and the ambiguity can be resolved [22] for the major part of the data by making use of the precise space point measurements provided by OPAL's 3-coordinate microvertex detector [13] installed in 1993. For  $\tau^+\tau^- \rightarrow \pi^+\bar{\nu}_\tau\pi^-\nu_\tau$  events the direction ambiguity can be resolved in about 80% of the cases. Out of those the correct solution is found with 77% probability. If the ambiguity cannot be resolved and in cases (b) and (c) both possible solutions are used to calculate two values for  $\mathcal{O}$ , which are then averaged. The precision with which the  $\tau$  flight direction can be reconstructed with and without resolving the ambiguity is compared in fig. 1.

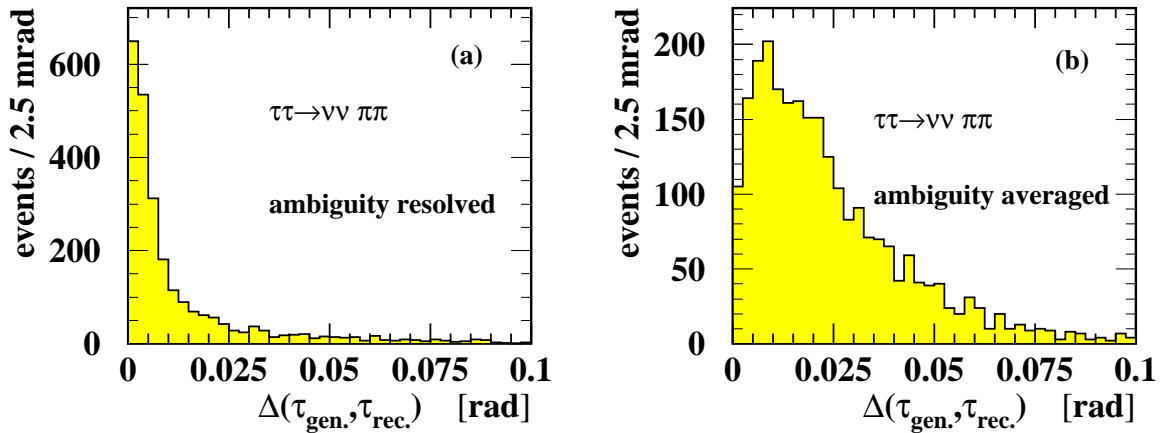


Figure 1: Reconstruction of the  $\tau$  flight direction. Shown is the distribution of the angle  $\Delta$  between the reconstructed and the true  $\tau$  direction in three dimensions found from simulated events. In (a) the ambiguity has been resolved, while in (b) an average of the two possible solutions is taken for the same events.

The spin vectors  $\mathbf{S}$  in the two  $\tau$  rest frames are estimated from the measured momenta of the  $\tau$  decay products. The partial decay width for any decay mode is given by the expression [23]

$$d\Gamma \propto 1 + \mathbf{h} \cdot \mathbf{S} \quad , \quad (4)$$

where  $\mathbf{h}$  is the so-called polarimeter vector which is a function of the momenta and energies of the  $\tau$  daughters and of the  $\tau$  flight direction. For a given spin vector  $\mathbf{S}$  the configuration with  $\mathbf{h}$  pointing in the direction of  $\mathbf{S}$  is the most likely one. Thus the best estimate of the spin direction is the direction of  $\mathbf{h}$  for which  $d\Gamma$  is maximal. Spin and polarimeter vectors for the different decay modes have been calculated in [14, 24] and are given in appendix C. For a perfect detector the spin analysing power would be the same for all hadronic  $\tau$  decays. Due to the reconstruction quality and the detector resolution the sensitivities are lower than the ideal values, particularly for decays including neutral pions. They also vary between the different decay channels (see section 5). For leptonic decays the estimate of  $\mathbf{S}$  is much less efficient because two neutrinos escape undetected.

## 5 The Sensitivities

The better the spin analysing power and the quality of the reconstruction of the  $\tau$  flight direction are for a given decay mode, the larger is the sensitivity of that final state to detect a possible  $\mathcal{CP}$  violating effect. The sensitivities  $c_{AB}$  and  $f_{AB}$  of eq. (1) and (2) are largest for those hadronic decays which allow a full reconstruction of the flight direction of the tau and they are smallest for leptonic tau decays.

In the following we successively determine (a) ‘pure’ sensitivities which already account for topological and kinematic cuts in the event selection, (b) ‘corrected’ sensitivities which take into account effects due to radiative corrections, uncertainties in  $\sin^2 \theta_W$ ,  $m_Z$  and  $m_\tau$  as well as the influence of finite energy and momentum resolution of the detector, and (c) ‘effective’ sensitivities which also include the effect of the background contamination in the selected event classes.

The ‘pure’ sensitivities are calculated using a Monte Carlo generator which includes a  $\mathcal{CP}$  violating amplitude on the generator level [24]. The ‘corrected’ sensitivities are determined by comparing the distribution of the observables using the particle four-momenta at MC-generator level with those using the momenta taken from the full detector simulation. A non-vanishing dipole moment is introduced into the Monte Carlo (KORALZ[25], TAUOLA [26]) including full detector simulation [27] by applying a reweighting method on an individual event basis transferring event weights from the generator level  $\mathcal{CP}$  Monte Carlo. The largest sensitivity loss is found for  $\tau$  decays including neutral hadrons while the influence of radiative corrections and Standard Model parameters on  $c_{AB}$  and  $f_{AB}$  are found to be less than 1.5%. Finally, the ‘effective’ sensitivities are determined under the assumption that the non- $\tau$  background is  $\mathcal{CP}$  symmetric. For  $e^+e^-$  and  $\mu^+\mu^-$  pair production, in particular, it has been pointed out in [5] that the expectation values for all  $\mathcal{CP}$ -odd observables are zero even if non-vanishing dipole moments of  $e$  or  $\mu$  exist. Background from the misidentification of  $\tau$  decay channels reduces the sensitivities since non-optimal observables are being used in this case. The largest sensitivity reduction is observed when  $\tau \rightarrow \rho\nu_\tau$  is misidentified as  $\tau \rightarrow \pi\nu_\tau$  and the neutral pion is ignored in calculating the observables. The systematic error includes the uncertainties in the determination of the background sources. Figure 2 shows the sensitivities  $c_{AB}$  and  $f_{AB}$  for all decay channels considered using the nomenclature defined above.

## 6 Test of the $\mathcal{CP}$ Symmetry of the Detector

The  $\mathcal{CP}$  symmetry of the OPAL detector is vital for this measurement. Detector effects may cause systematic shifts of the expectation values of the observables  $\mathcal{O}_{AB}$  and can thus fake  $\mathcal{CP}$  violation or even hide a real  $\mathcal{CP}$  violation effect. The level of  $\mathcal{CP}$  symmetry of the detector must therefore be quantified and included in the systematic error of the measurement. Expanding the expressions of the  $\mathcal{CP}$  violating contributions to the squared amplitude in eq. (3) in polar coordinates one finds that the

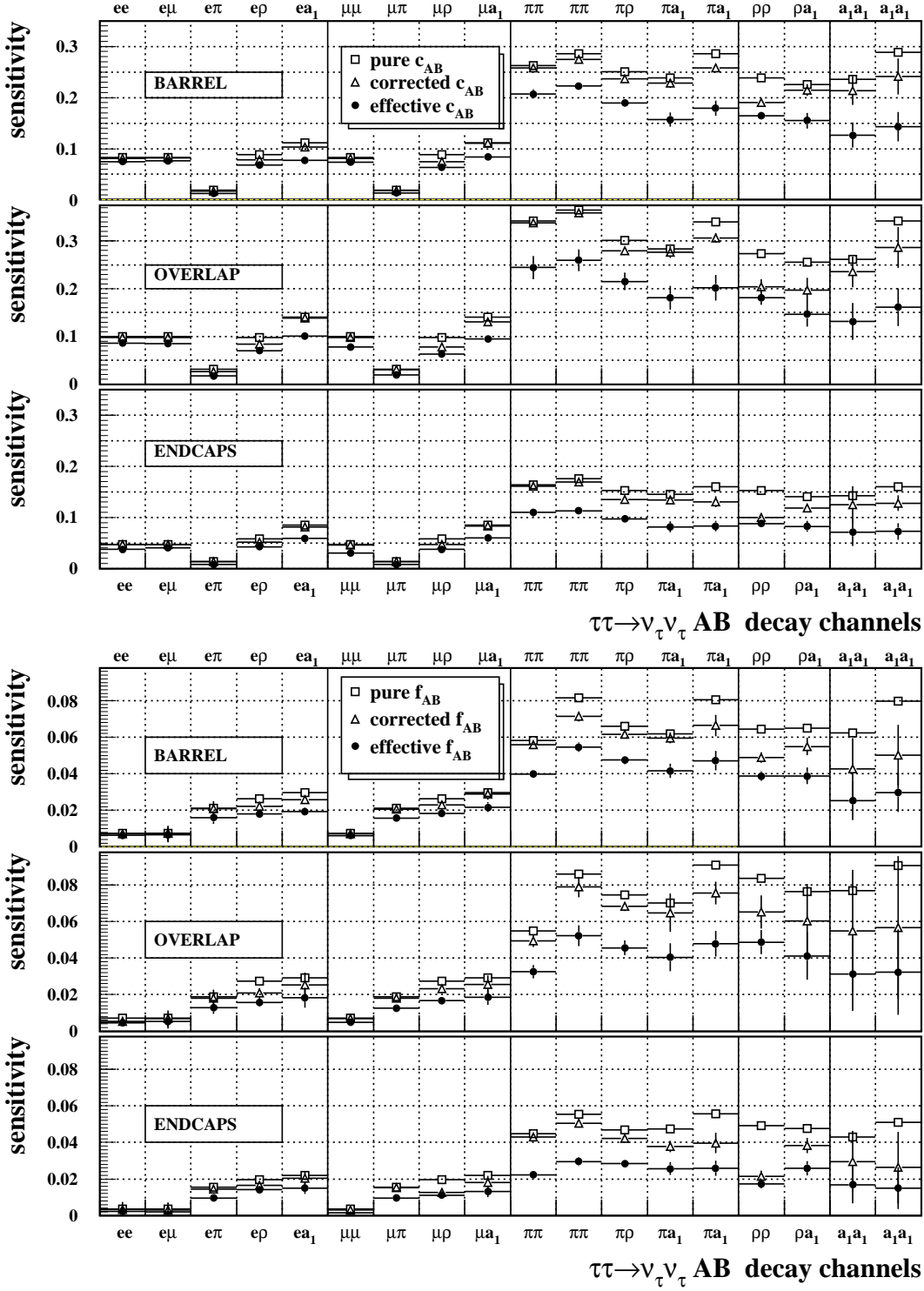


Figure 2: *Pure* (including phase space cuts), *corrected* (including the finite resolution and detector effects) and *effective* (including the backgrounds) sensitivities  $c_{AB}$  for the  $T$ -odd observables (top) and  $f_{AB}$  for the  $T$ -even observables (bottom). Decay topologies which appear twice refer to different data taking periods, the first column being for the run periods 1991 and 1992 without resolving the ambiguity and the second for the run period 1993 - 1995, where the ambiguity is resolved using the information of the 3-coordinate microvertex detector.

leading terms of  $\mathcal{M}_{\mathcal{CP}}^{\text{Re}}$  are proportional to  $\sin(\phi^+ - \phi^-)$ , where  $\phi^\pm$  is the azimuthal angle of a given  $\tau^\pm$  decay product ( $e, \pi, \rho, a_1$ ), and the leading terms of  $\mathcal{M}_{\mathcal{CP}}^{\text{Im}}$  are proportional to  $\cos(\theta^+ - \theta^-)$ , where  $\theta^\pm$  is the decay product's polar angle.  $\mathcal{CP}$  violation can thus be faked by measuring particle directions systematically wrongly, caused for example by a misalignment of detector components such as a possible systematic rotation of the drift chamber end flanges or the endcaps or by systematically biased reconstruction algorithms. Other sources, which may lead to systematic shifts of the expectation values, are local detector defects or charge dependent identification probabilities.

In order to investigate these effects we have studied events for which non-vanishing expectation values of  $\mathcal{O}$  arising from a true  $\mathcal{CP}$  violation can be definitively excluded. Such events can be artificially constructed destroying the  $\tau$  spin correlations by combining  $\tau$  decays from different events with similar event topologies. In doing so, one must carefully avoid not to average out possible  $\mathcal{CP}$  biases of the detector, which, for example, would occur when events were simply mixed at random. We therefore combine a 1-prong tau decay (decay no. 1) in a given event with the  $\tau$  decay cone from another event also recoiling against a 1-prong  $\tau$  decay (decay no. 2) if and only if the tracks of decays no. 1 and no. 2 coincide within a small angle and have the same charge. For 3-prong decays the same requirement is made for the vector sum of the track momenta.

We have verified that the spin correlations are indeed destroyed by this procedure using simulated events which were generated with a non-vanishing dipole moment. A systematic, detector induced  $\mathcal{CP}$  asymmetry, however, survives this treatment as has been checked by introducing a systematic distortion of tracks in the detector.

Applying this mixing procedure to the data we find that the expectation values of all  $\mathcal{CP}$  observables are either consistent with zero or small and negligible compared to the measurement reported here. Quadratically adding the deviation of the mean value from zero with its error, using several hundred thousand artificial events for every decay channel, we conclude that the detector is  $\mathcal{CP}$  symmetric to a level of  $|\text{Re}(d_\tau^w)| < 0.5 \times 10^{-18} e \text{ cm}$  and  $|\text{Im}(d_\tau^w)| < 0.9 \times 10^{-18} e \text{ cm}$ , respectively, at 95% confidence level. The influence of this possible detector imperfection on the ability to measure  $d_\tau^w$  has been added to the systematic error. It constitutes the main contribution to the systematics of this measurement, but is small compared to the statistical precision.

## 7 Results and Conclusions

From the data samples recorded between 1991 and 1995 with OPAL, 69778  $\tau$ -pair events have been selected in the decay channels used in this analysis. Employing equations (1) and (2) the real and imaginary parts of the weak dipole moment are determined from the mean values of the  $\mathcal{CP}$ -odd observables for the different decay topologies and detector regions. In order to avoid effects of detector resolution tails on the measurements, the means are calculated in restricted regions of the values of the observables. These trim regions are defined such that the loss of sensitivity of the observable from excluding values outside the region is predicted by Monte Carlo to be minimal. The results are insensitive to the exact values of the trims. The measured dipole moments, separated by topology and detector region, are plotted in fig. 3. The systematic errors, which are also limited by finite statistics, are small compared to the statistical errors for the individual measurements. The final results are the error weighted averages of the individual measurements. The total systematic error includes the uncertainties in determining the sensitivities as well as the  $\mathcal{CP}$  symmetry of the detector. For the real and imaginary parts of the weak dipole moment we obtain

$$\begin{aligned} \text{Re}(d_\tau^w) &= (0.72 \pm 2.46 \pm 0.24) \times 10^{-18} e \text{ cm} \\ \text{Im}(d_\tau^w) &= (0.35 \pm 0.57 \pm 0.08) \times 10^{-17} e \text{ cm} \end{aligned}$$

where the first error is statistical and the second due to systematic uncertainties. Both measurements are consistent with zero, resulting in the upper limits

$$|\text{Re}(d_\tau^w)| < 5.6 \times 10^{-18} e \text{ cm}$$

$$\begin{aligned} |\text{Im}(d_\tau^w)| &< 1.5 \times 10^{-17} e \text{ cm} \\ |d_\tau^w| &< 1.6 \times 10^{-17} e \text{ cm} \end{aligned}$$

at 95% confidence level which can be compared to the level of a few  $10^{-19} e \text{ cm}$  predicted by some models.

In order to assess the relative importance of this result one may consider models with a  $\mathcal{CP}$  violating Higgs sector [6] or with leptoquarks [8]. Assuming that weak and electric dipole moments can be directly compared and have roughly the same magnitude [6, 8], we have scaled the above result for  $|d_\tau^w|$  with the ratio of fermion masses<sup>2</sup> in table 3. For the case of the electron this simple scaling is an oversimplification. Other models [28] also exist which predict a weaker dependence on the mass of

|          | measured<br>$d^{electric}$ [29]    | predicted from $ d_\tau^w $      |                                  |
|----------|------------------------------------|----------------------------------|----------------------------------|
|          |                                    | multi-Higgs models               | leptoquark models                |
| Electron | $1.9 \times 10^{-26} e \text{ cm}$ | $5 \times 10^{-28} e \text{ cm}$ | $5 \times 10^{-30} e \text{ cm}$ |
| Muon     | $1.0 \times 10^{-18} e \text{ cm}$ | $5 \times 10^{-21} e \text{ cm}$ | $5 \times 10^{-23} e \text{ cm}$ |

Table 3: Comparison of limits on dipole moments from direct measurements with scaled limits from  $|d_\tau^w|$  from this analysis for mass dependences as obtained in multi-Higgs models ( $d_f \propto m_f^3$ ) and in leptoquark models ( $d_\tau : d_\mu : d_e = m_\tau m_t^2 : m_\mu m_c^2 : m_e m_u^2$ ), respectively.

the fermion. Nevertheless, table 1 indicates that in terms of certain model expectations, the present limit on  $d_\tau^w$  is more restrictive than existing measurements on the electric dipole moment of electron and muon, respectively.

Another useful assessment of our result can be obtained by defining an  $\epsilon$  parameter as

$$\epsilon_\tau \equiv \frac{\Delta\Gamma_{Z^0 \rightarrow \tau^+ \tau^-}}{\Gamma_{Z^0 \rightarrow \tau^+ \tau^-}} \quad , \quad \text{where} \quad \Delta\Gamma_{Z^0 \rightarrow \tau^+ \tau^-} = \frac{|d_\tau^w|^2}{24\pi} m_Z^3 \left(1 - \frac{4m_\tau^2}{m_Z^2}\right)^{3/2}$$

is the additional contribution to  $\Gamma_{Z^0 \rightarrow \tau^+ \tau^-}$  due to the new  $\mathcal{CP}$  violating interaction. Using our limits on  $|d_\tau^w|$  and on  $|\text{Re}(d_\tau^w)|$  and  $\Gamma_{Z^0 \rightarrow \tau^+ \tau^-} = (83.88 \pm 0.39) \text{ MeV}$  [29]<sup>3</sup> one obtains

$$\begin{aligned} \epsilon_\tau &< 7.2 \times 10^{-3} && \text{using } |d_\tau^w| && \text{and} \\ \epsilon_\tau &< 8.9 \times 10^{-4} && \text{assuming } \text{Im}(d_\tau^w) = 0 \end{aligned}$$

at 95% C.L. The above limits on  $\epsilon_\tau$  indicate that the precision of the test of  $\mathcal{CP}$  invariance in  $Z^0 \rightarrow \tau^+ \tau^-$  has reached a level of one in thousand.

<sup>2</sup>The values used for the quark masses are  $m_u = 5 \text{ MeV}$ ,  $m_c = 1.3 \text{ GeV}$ ,  $m_t = 180 \text{ GeV}$ .

<sup>3</sup>The value for  $\Gamma_{Z^0 \rightarrow \tau^+ \tau^-}$  used here is  $\Gamma_{\text{tot}} \times \text{B}_{\tau\tau}$  where  $\Gamma_{\text{tot}} = 2496.3 \pm 3.2 \text{ MeV}$  is the total width as determined from a global SM fit (see ref.[29]).

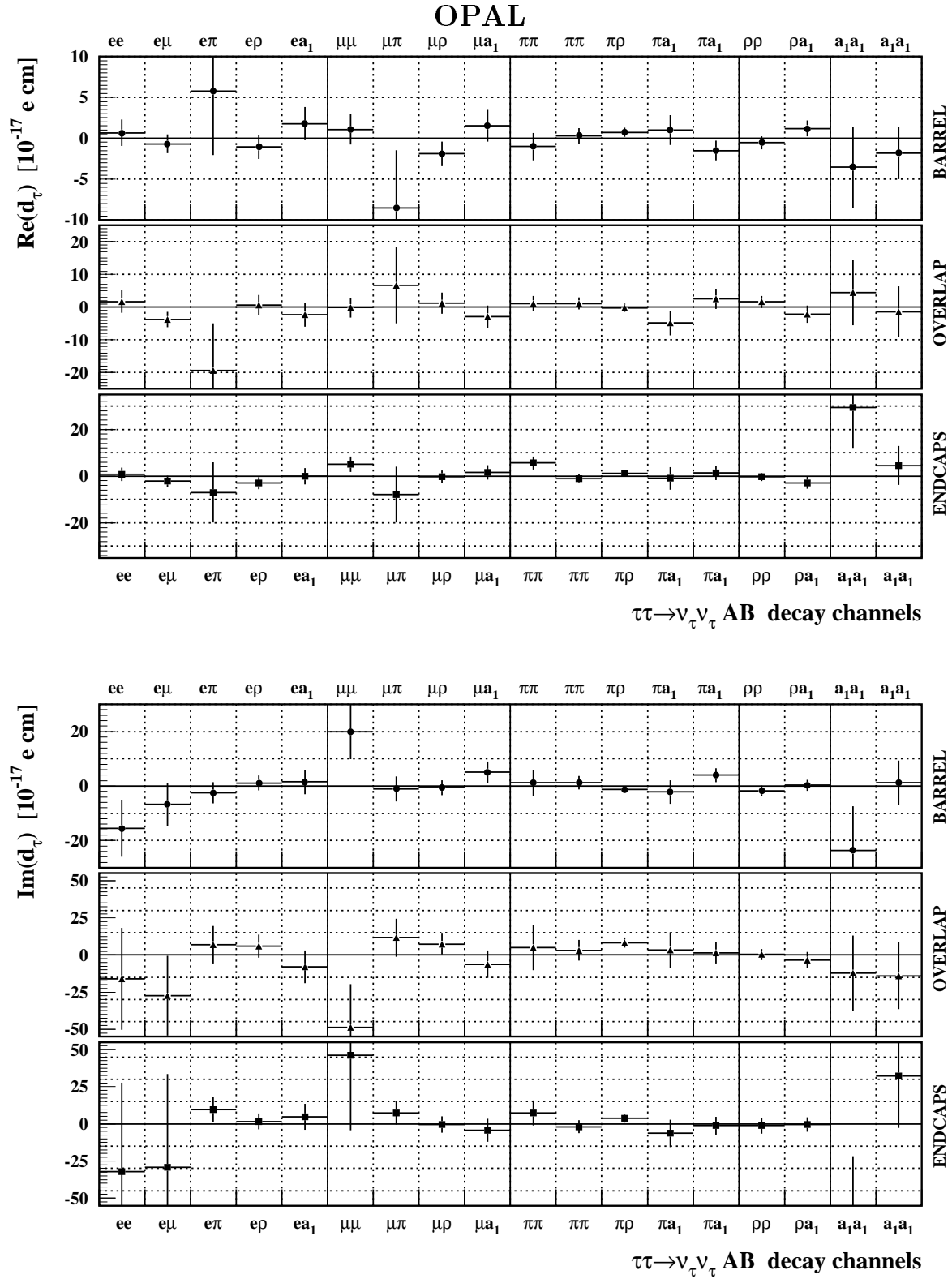


Figure 3: Real part (top) and imaginary part (bottom) of the weak dipole moment of the tau for the different decay topologies and detector regions.

## Acknowledgements

We gratefully acknowledge numerous helpful discussions with P. Overmann, W. Bernreuther, O. Nachtmann, J. H. Kühn, M. Wunsch and A. Höcker.

It is a pleasure to thank the SL Division for the efficient operation of the LEP accelerator and for their continuing close cooperation with our experimental group. In addition to the support staff at our own institutions we are pleased to acknowledge the

Department of Energy, USA,

National Science Foundation, USA,

Particle Physics and Astronomy Research Council, UK,

Natural Sciences and Engineering Research Council, Canada,

Israel Science Foundation, administered by the Israel Academy of Science and Humanities,

Minerva Gesellschaft,

Japanese Ministry of Education, Science and Culture (the Monbusho) and a grant under the Monbusho International Science Research Program,

German Israeli Bi-national Science Foundation (GIF),

Direction des Sciences de la Matière du Commissariat à l'Énergie Atomique, France,

Bundesministerium für Bildung, Wissenschaft, Forschung und Technologie, Germany,

National Research Council of Canada,

Hungarian Foundation for Scientific Research, OTKA T-016660, and OTKA F-015089.

## Appendix A: Squared Amplitudes

Neglecting all terms proportional to the small neutral current vector couplings of leptons,  $g_V$ , in the  $\tau$  pair spin density matrix [17], the leading terms of the squared amplitudes in eq. (3) are given by

$$\mathcal{M}_{\mathcal{CP}}^{\text{Re}} = (\hat{\mathbf{k}} \cdot \hat{\mathbf{q}}_e) \left( \hat{\mathbf{k}} \times (\mathbf{S}^+ - \mathbf{S}^-) \right) \cdot \hat{\mathbf{q}}_e$$

$$\mathcal{M}_{\mathcal{CP}}^{\text{Im}} = (\hat{\mathbf{k}} \cdot \hat{\mathbf{q}}_e) \left[ (\hat{\mathbf{k}} \cdot \mathbf{S}^-)(\hat{\mathbf{q}}_e \cdot \mathbf{S}^+) - (\hat{\mathbf{k}} \cdot \mathbf{S}^+)(\hat{\mathbf{q}}_e \cdot \mathbf{S}^-) \right]$$

$$\begin{aligned} \mathcal{M}_{SM} = & 1 + (\hat{\mathbf{k}} \cdot \hat{\mathbf{q}}_e)^2 + \mathbf{S}^+ \cdot \mathbf{S}^- (1 - (\hat{\mathbf{k}} \cdot \hat{\mathbf{q}}_e)^2) - 2(\hat{\mathbf{q}}_e \cdot \mathbf{S}^+)(\hat{\mathbf{q}}_e \cdot \mathbf{S}^-) \\ & + 2(\hat{\mathbf{k}} \cdot \hat{\mathbf{q}}_e) \left[ (\hat{\mathbf{k}} \cdot \mathbf{S}^+)(\hat{\mathbf{q}}_e \cdot \mathbf{S}^-) + (\hat{\mathbf{k}} \cdot \mathbf{S}^-)(\hat{\mathbf{q}}_e \cdot \mathbf{S}^+) \right]. \end{aligned}$$

Here  $\hat{\mathbf{q}}_e$  is the direction of the incoming electron,  $\hat{\mathbf{k}}$  the flight direction of the  $\tau^+$ , and  $\mathbf{S}^\pm$  are the spin vectors of the  $\tau^\pm$  leptons in their respective rest systems.

## Appendix B : Tau Flight Direction

Considering the reaction  $e^+e^- \rightarrow \tau^+(\hat{\mathbf{k}})\tau^-(-\hat{\mathbf{k}}) \rightarrow A^+(E_A, \mathbf{p}_A)B^-(E_B, \mathbf{p}_B)\nu_\tau\bar{\nu}_\tau$  the direction unit vector of the  $\tau^+$  is given by:

$$\hat{\mathbf{k}} = u\hat{\mathbf{p}}_A + v\hat{\mathbf{p}}_B \pm w \frac{(\mathbf{p}_A \times \mathbf{p}_B)}{|\mathbf{p}_A \times \mathbf{p}_B|},$$

where hats denote unit momenta in the laboratory frame. The two solutions differ only by the sign of the component  $w$  perpendicular to the decay plane.  $u$ ,  $v$  and  $w$  can be calculated as

$$\begin{aligned} u = \frac{\cos\theta_A + \hat{\mathbf{p}}_A \cdot \hat{\mathbf{p}}_B \cos\theta_B}{1 - (\hat{\mathbf{p}}_A \cdot \hat{\mathbf{p}}_B)^2} \quad v = -\frac{\cos\theta_B + \hat{\mathbf{p}}_A \cdot \hat{\mathbf{p}}_B \cos\theta_A}{1 - (\hat{\mathbf{p}}_A \cdot \hat{\mathbf{p}}_B)^2} \\ w = \sqrt{1 - u^2 - v^2 - 2uv(\hat{\mathbf{p}}_A \cdot \hat{\mathbf{p}}_B)}, \end{aligned}$$

where  $\theta_{A/B}$  is the angle between the tau momenta and the momenta of the daughters A,B

$$\cos \theta_{A/B} = \frac{2E_\tau E_{A/B} - m_{A/B}^2 - m_\tau^2}{2|\mathbf{p}_{A/B}||\mathbf{k}_\tau|}.$$

Three different cases must be considered in the reconstruction.

(i) *Both taus decay to charged hadrons only.*

For event topologies including the decays  $\tau \rightarrow \pi^\pm \nu_\tau$  or  $\tau \rightarrow 3\pi^\pm \nu_\tau$  in both hemispheres the ambiguity can be resolved by calculating the vector of the minimal distance in space,  $\mathbf{d}_{min}$ , between the tracks of the  $\tau$  products as proposed by Kühn [22]. The orientation of  $\mathbf{d}_{min}$  relative to the normal to the decay plane determines the sign of  $w$  and thus allows the calculation of the correct solution for the  $\tau$  direction. For 3-prong decays the momentum sum vector together with the vertex information of the three tracks is used for this construction. The information from the new, 3-coordinate silicon microvertex detector [13], which provides very precise space point measurements close to the interaction point in  $r$ - $\phi$  and  $z$ , allows the correct solution to be found with an efficiency substantially larger than 50%, which is the value if no reconstruction is attempted.

(ii) *Both taus decay to hadrons, but at least one neutral hadron is contained in the final state.*

For these topologies the  $\tau$  direction can be calculated up to the twofold ambiguity as mentioned above. The ambiguity cannot be resolved because the flight path (in space) of the neutral hadrons cannot be reconstructed with the required accuracy.

(iii) *One or both taus decay to leptons only.*

In this case the equation for  $\cos \theta_{A/B}$  is not quite correct but includes instead the invariant mass of the two unobserved neutrinos in the numerator. Because the latter cannot be measured we neglect this mass here and perform an approximate reconstruction.

## Appendix C: Spin Formulae

This appendix summarises the formulae for estimating the spin vectors [14, 24].

The four-momenta of the taus are denoted by:  $\mathbf{k}^\pm = (E_\tau, \pm \mathbf{k})$ .

- $\tau \rightarrow \ell \nu_\tau$

$$\mathbf{S}_{\tau \rightarrow \ell \nu_\tau}^\pm = \pm \frac{(m_\tau \mathbf{p}_{\ell^\pm} \mp (E_{\ell^\pm} \mp (\mathbf{p}_{\ell^\pm} \cdot \mathbf{k}) / (E_\tau + m_\tau)) \mathbf{k}) (4\mathbf{p}_{\ell^\pm} \cdot \mathbf{k}^\pm - m_\tau^2 - 3m_\ell^2)}{\mathbf{p}_{\ell^\pm} \cdot \mathbf{k}^\pm (3m_\tau^2 + 3m_\ell^2 - 4\mathbf{p}_{\ell^\pm} \cdot \mathbf{k}^\pm) - 2m_\ell^2 m_\tau^2}$$

where  $\mathbf{p}_{\ell^\pm} = (E_{\ell^\pm}, \mathbf{p}_{\ell^\pm})$  is the four-momentum of the outgoing lepton. Note that the form of this expression is somewhat different than that used, incorrectly, in ref. [11]. The results obtained in ref [11] remain valid, however, as the incorrect calculation used there only reduces the sensitivity of the leptonic observable compared to the optimal value which is obtained from the correct form of  $\mathbf{S}_{\tau \rightarrow \ell \nu_\tau}^\pm$  given above.

- $\tau \rightarrow \pi \nu_\tau$

$$\mathbf{S}_{\tau \rightarrow \pi \nu}^\pm = \frac{2}{m_\tau^2 - m_\pi^2} \left( \mp m_\tau \mathbf{p}_{\pi^\pm} + \frac{m_\tau^2 + m_\pi^2 + 2m_\tau E_{\pi^\pm}}{2(E_\tau + m_\tau)} \mathbf{k} \right)$$

where  $\mathbf{p}_{\pi^\pm} = (E_{\pi^\pm}, \mathbf{p}_{\pi^\pm})$  denotes the pion's four-momentum.

- $\tau \rightarrow \rho \nu_\tau \rightarrow \pi \pi^0 \nu_\tau$

$$\mathbf{S}_{\tau \rightarrow \pi \pi^0 \nu}^\pm = \mp \frac{\mp (\mathbf{H}^\pm)^0 \mathbf{k} + m_\tau \mathbf{H}^\pm + \mathbf{k}(\mathbf{k} \cdot \mathbf{H}^\pm) / (E_\tau + m_\tau)}{(\mathbf{k}_\pm \cdot \mathbf{H}^\pm) - m_\tau^2 (\mathbf{p}_{\pi^\pm} - \mathbf{p}_{\pi^0})^2}$$

with

$$(\mathbf{H}^\pm)^\nu = 2(\mathbf{p}_{\pi^\pm} - \mathbf{p}_{\pi^0})^\nu (\mathbf{p}_{\pi^\pm} - \mathbf{p}_{\pi^0})^\mu (\mathbf{k}_\pm)_\mu + (\mathbf{p}_{\pi^\pm} + \mathbf{p}_{\pi^0})^\nu (\mathbf{p}_{\pi^\pm} - \mathbf{p}_{\pi^0})^2$$

where  $\mathbf{p}_{\pi^\pm}$  and  $\mathbf{p}_{\pi^0}$  are the four-momenta of charged and neutral pion.

- $\tau \rightarrow \mathbf{a}_1 \nu_\tau \rightarrow \pi \pi \pi \nu_\tau$

With the following notations

$$\tau^\pm(0) \rightarrow \mathbf{a}_1^\pm(Q) \nu_\tau(q), \quad \mathbf{a}_1^\pm(Q) \rightarrow \pi^\mp(p) \pi^\pm(p_1) \pi^\pm(p_2), \quad u_{1/2} = (p + p_{1/2})^2$$

in the tau rest-frame we get:

$$\mathbf{S}_{\tau \rightarrow 3\pi}^\pm = \mp \frac{\mathbf{P}}{p_0}$$

where

$$\begin{aligned} \mathbf{P}^\mu &= \text{Re}(\text{BW}(u_1)\text{BW}(u_2)^*) (2m_\tau h_1^0 h_1^\mu - q^\mu (h_1)^2) \\ &+ \text{Re}(\text{BW}(u_2)\text{BW}(u_2)^*) (2m_\tau h_2^0 h_2^\mu - q^\mu (h_2)^2) \\ &+ 2\text{Re}(\text{BW}(u_1)\text{BW}(u_2)^*) (m_\tau (h_1^0 h_2^\mu + h_2^0 h_1^\mu) - q^\mu h_1^\nu h_{2\nu}) \\ &+ 2\text{Im}(\text{BW}(u_1)\text{BW}(u_2)^*) \mathbf{F}^\mu \end{aligned}$$

$$\mathbf{F}^\mu = - \begin{pmatrix} q^1 g^{23} + q^2 g^{31} + q^3 g^{12} \\ q^0 g^{23} + q^2 g^{30} + q^3 g^{02} \\ q^1 g^{03} + q^0 g^{31} + q^3 g^{10} \\ q^1 g^{20} + q^2 g^{01} + q^0 g^{12} \end{pmatrix} \quad \begin{aligned} h_{1/2}^\mu &= (p - p_{1/2})^\mu - Q^\mu \left( \frac{Q^\nu (p - p_{1/2})_\nu}{Q^2} \right) \\ g^{\mu\nu} &= h_1^\mu h_2^\nu - h_1^\nu h_2^\mu \end{aligned}$$

with the Breit-Wigner propagator :

$$\text{BW}(u) = \frac{m_\rho^2}{m_\rho^2 - u - i\sqrt{u}\Gamma(u)}$$

and the momentum dependent, p-wave corrected width:

$$\Gamma(u) = \Gamma_\rho \frac{m_\rho^2}{u} \left( \frac{u - 4m_\pi^2}{m_\rho^2 - 4m_\pi^2} \right)^{3/2}$$

## References

- [1] A. D. Sakharov, *JETP Lett.* **5**, 24 (1967).
- [2] J. H. Christensen et al., *Phys. Rev. Lett.* **13**, 138 (1964).
- [3] M. Kobayashi and T. Maskawa, *Prog. Theor. Phys.* **49**, 652 (1973)
- [4] P. Huet and E. Sather, *Phys. Rev.* **D 51**, 279 (1995);  
M. B. Gavela, *Nucl. Phys.* **B 430**, 345 (1994),
- [5] W. Bernreuther, U. Löw, J. P. Ma and O. Nachtmann, *Z. Phys.* **C 43** (1989) 117.
- [6] W. Bernreuther and O. Nachtmann, *Phys. Rev. Lett.* **63** (1989) 2787.
- [7] S. Barr and A. Zee, *Phys. Rev. Lett.* **65** (1990) 21.

- [8] W. Bernreuther, A. Brandenburg and P. Overmann ‘CP Violation Beyond the SM and Tau Pair Production in  $e^+e^-$  Collisions’, PITHA-96-26 (1996).
- [9] W. Bernreuther and O. Nachtmann, ‘Some Remarks on the Search for  $\mathcal{CP}$  Violation in Z-decays’, HD-THEP-96-03 (1996).
- [10] OPAL Collaboration, P. D. Acton et al., *Phys. Lett.* **B 281** (1992) 405.
- [11] OPAL Collaboration, R. Akers et al., *Z. Phys.* **C 66** (1995) 31.
- [12] ALEPH Collaboration, D. Buskulic et al., *Phys. Lett.* **B 297** (1992) 459; *Phys. Lett.* **B 371** (1995) 371;
- [13] P. P. Allport et al., *Nucl. Inst. and Meth.* **A 346** (1994) 476.
- [14] P. Overmann, ‘A new method to measure the tau polarization at the Z peak.’, *Univ. of Dortmund: DO-TH 93-24*, (1993);  
P. Overmann, *Dissertation, Inst. f. theor. Physik, Heidelberg* (1992)
- [15] D. Atwood and A. Soni, *Phys. Rev.* **D 45** (1992) 2405.
- [16] M. Diehl and O. Nachtmann, *Z. Phys.* **C 62** (1994) 397.
- [17] W. Bernreuther, O. Nachtmann and P. Overmann, *Phys. Rev.* **D 48** (1993) 78.
- [18] OPAL Collaboration, K. Ahmet et al., *Nucl. Inst. and Meth.* **A 305** (1991) 275.
- [19] P. P. Allport et al., *Nucl. Inst. and Meth.* **A 324** (1993) 34.
- [20] OPAL Collaboration, R. Akers et al., *Phys. Lett.* **B 328** (1994) 207.
- [21] M. Thomson CERN-PPE (96-055) (1996) accepted by *Nucl. Inst. and Meth..*
- [22] J. H. Kühn, *Phys. Lett.* **B 313** (1993) 458.
- [23] Y. S. Tsai, *Phys. Rev.* **D 4** (1971) 2821.
- [24] P. Overmann, Inst. f. Theor. Physik, Univ. Heidelberg, private communication.
- [25] S. Jadach, B. F. L. Ward and Z. Was, *Comp. Phys. Comm.* **66** (1991) 276.
- [26] S. Jadach, J. H. Kühn and Z. Was, *Comp. Phys. Comm.* **64** (1991) 275.
- [27] J. Allison et al., *Nucl. Inst. and Meth.* **A 317** (1992) 47.
- [28] Hai-Yang Cheng, *Phys. Rev.* **D 28** (1983) 150.
- [29] Particle Data Group, R. M. Barnett et al., *Phys. Rev.* **D 54** (1996) 1.